Vision Res. Vol. 32, No. 6, pp. 1099–1113, 1992
Printed in Great Britain. All rights reserved

0042-6989/92 $5.00 + 0.00
Copyright © 1992 Pergamon Press Ltd

Extraocular Muscle Forces in Alert Monkey

JOEL M. MILLER,* DAVID ROBINS*†

Received 18 July 1991; in revised form 30 October 1991

We describe an extraocular muscle (EOM) force transducer that provides low-noise signals from an alert animal for several months, is implanted without disinserting the muscle, and is well-tolerated by the body, and present results obtained with the device. The transducer can be used to study orbital statics and dynamics, and oculomotor control signals undiminished by orbital low-pass filtering and antagonistic pairing of muscles. It may provide an index of effective EOM innervation, useful in studies of orbital tissue healing and plasticity, and oculomotor (OM) signal adaptation. During horizontal saccades transducers implanted in the lateral rectus (LR) and medial rectus (MR) of a monkey trained to fixate revealed an agonist muscle tension waveform corresponding to the "pulse-slide-step" pattern of saccadic innervation, and an antagonist waveform that was similar within a scale factor. We never observed transient increases in antagonist force at the ends of saccades (active braking) or at the beginnings. Onset of saccadic force in LR preceded that in MR by 1.6 msec for abducting saccades, and lagged that in MR by 1.1 msec for adducting saccades. During vertical saccades, transient force changes were found in LR and MR, which were likely due, at least in part, to globe translation. LR and MR forces during fixation tended to be largest with the eye about 10° in elevation, and smallest in depression, indicating that effective total innervation was a function of vertical gaze, or that there was variation in the elastic component of muscle force related to orbital geometry, with LR and MR innervation independent of vertical gaze. An exponential decrease in fixation force, having a time constant of about 10 days, was observed after implantation. This may have reflected adaptive muscle lengthening or post-surgical healing.

Chronic implant Extraocular muscle Eye movement Force transducer Monkey Muscle force Oculomotility Saccade

INTRODUCTION

Oculomotor physiologists routinely measure eye position and brainstem neural activity, but are unable to measure the forces produced by the muscles, the "motors" themselves. For some purposes electromyograms (EMG) are useful indices of muscle force. However, EMG does not measure muscle force, reflect a representative sample of motor units, or yield signals stable enough to study slow changes, such as those associated with post-surgical healing and adaptive processes. Muscle forces contain more information about oculomotor control signals than do eye position measurements, because eye rotation is low-pass filtered by the orbit's mechanics (Robinson, 1964), and has half the degrees of freedom of muscle forces, due to the antagonistic pairing of muscles.

Three basic types of force transducer have been used to study the biomechanics of skeletal muscles: *E-form*, *buckle-form*, and *C-form*. Walmsley, Hodgson and Burke (1978) used an E-form device on cat soleus. The buckle-form transducer was originally introduced by Salmons (1969), and has been used on leg muscle tendons of horses and cats. A C-form transducer, small enough to use on an unrestrained eye, was developed and used acutely by Collins, O'Meara and Scott (1975) to record horizontal rectus muscle forces during fixations and eye movements in human volunteers undergoing strabismus surgery. The device was sutured at one end to a point on the sclera, and at the other to a point on the cut end of the muscle tendon, and was used to study eye movements in the plane of the operated muscle (e.g. horizontal movements with lateral rectus installation).

We sought to develop an extraocular muscle force transducer that would minimally disturb ocular mechanics, and deliver stable, high-resolution signals for several weeks or months. We did not consider the C-form design, since its implantation disturbs the eye's 3-dimensional mechanics by reducing the muscle's insertion line to a point, and the required tenectomy would cause scarring in a chronic preparation (Searl, Metz & Lindahl, 1987). We found the E-form design to be excessively sensitive to tendon alignment. The buckle-form device we describe in *Methods* approximates our

*Smith-Kettlewell Eye Research Institute, 2232 Webster Street, San Francisco, CA 94115, U.S.A.
†Present address: The Permanente Medical Group, Vallejo, CA 94589, U.S.A.

goals. In *Results* we present muscle force data collected with the first prototypes of the device, and analyses of these data that bear on several issues in oculomotor physiology.

METHODS

Transducer design

The plan of the extraocular muscle force transducer is shown in Fig. 1. Semiconductor strain gauges, selected for high sensitivity to strain, also have high sensitivity to temperature, such that a change of a few °C would produce a change in gauge resistance equal to that caused by the largest EOM force. An error correlated with eye position might thereby be introduced by the varying exposure of the device to external temperatures during eye rotation. Happily, a push–pull arrangement of two silicon elements provides temperature compensation, while increasing and linearizing transducer output. The completed transducer had a residual temperature sensitivity such that a change of 3 or 4°C mimicked a muscle force change of 1 g, small enough to ignore for our purposes.

An implanted silicon strain gauge must be coated to protect it from moisture. The coating must be uniform and its thickness controllable, since the mechanical properties of the device depend on its dimensions and stiffness. Parylene-C (poly-monochloro-para-xylylene: Union Carbide, Danbury, Conn.), a crystalline polymer, vapor-deposited at near room temperature, forms continuous coatings with excellent barrier properties on substrates of arbitrary shape, with thickness controlled to 10%. Parylene-C is highly biocompatible, which is critical to avoid foreign-body reaction, which would disturb orbital mechanics and, possibly, vision. It supports normal tissue growth, without granulation or scarring (Nichols & Hahn, 1987; Schmidt, McIntosh & Bak, 1988).

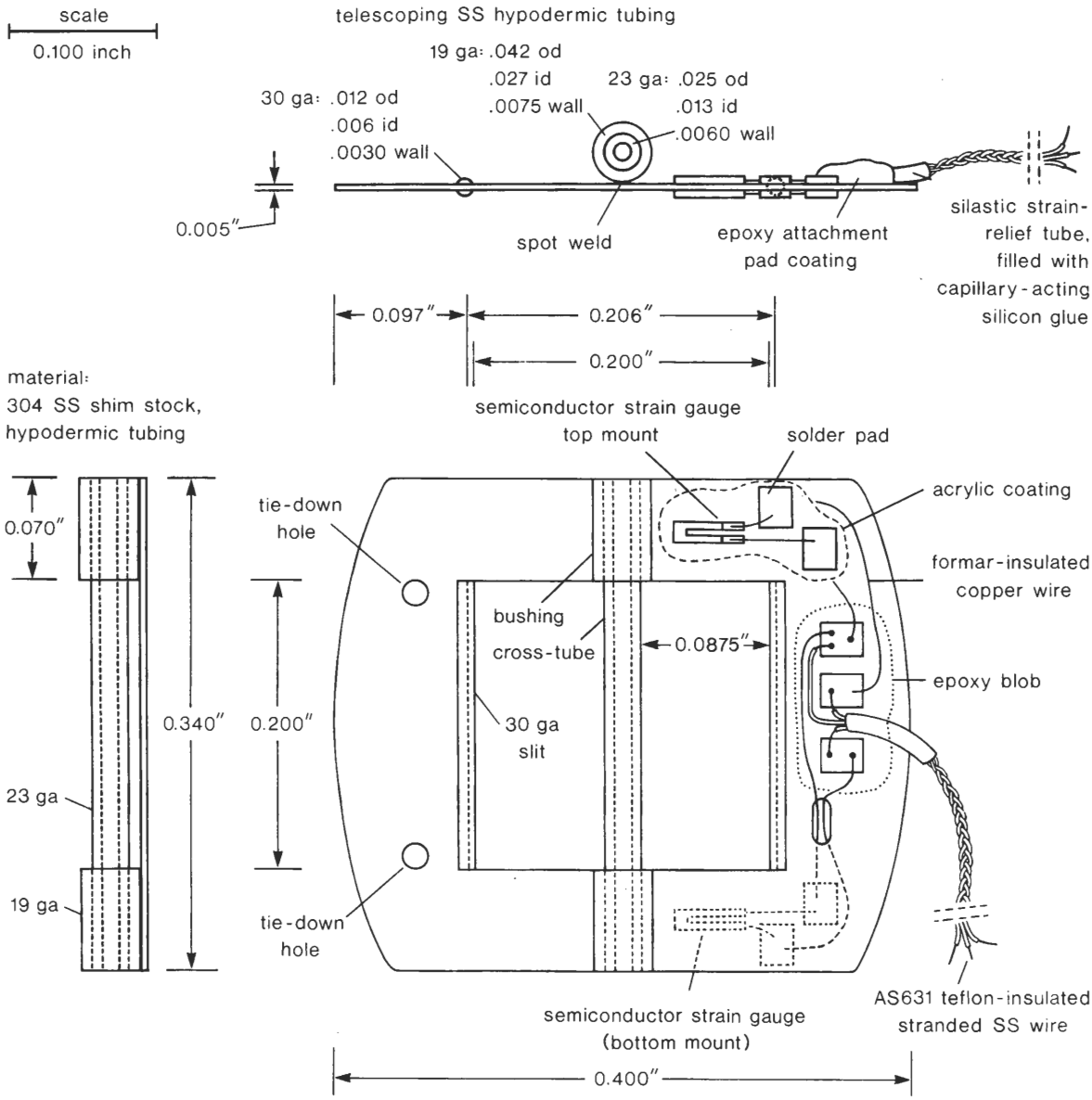

FIGURE 1. Transducer plan. This scale drawing shows the extraocular muscle force transducer in top view and two side views. See text for discussion.

A small device is less likely to interfere with normal eye movement or deform through contact with globe or orbit during eye rotation. For this prototype device, however, we did not attempt extreme miniaturization. The width of the transducer aperture (0.200 in) was chosen to fit monkey tendon (Miller & Robins, 1987). We also sought to cause only minimal lengthening of the muscle's path (~0.25 mm), and provide sufficient surface area for component mounting.

The bar-shaped sides of the transducer frame, or *beams*, bend in response to muscle force, stretching or compressing strain gauges bonded to their surfaces, thereby altering gauge resistance (Fig. 1). Typical of strain gauge applications, the amount of bending does not significantly alter frame geometry, which simplifies analysis and avoids a potential nonlinearity. The transducer may be considered as two *simple beams*, each beam having a solid rectangular cross-section and load concentrated at its center, joined at their ends by inflexible bars. Analysis of the beams is straightforward (see, e.g. Eshbach & Souders, 1975). We selected a beam width of 0.070 in to fit the silicon gauges and their solder pads, and a beam height of 0.005 in, so that, supposing a maximum muscle tension of 50 g, the bonds between gauges and substrate would be stressed to one-half of their creep limit.

Another benefit of isometric measurement is that any connective or scar tissue that forms around the transducer itself would have minimal effect on its performance. Although such tissue might be mechanically in parallel with the transducer, its stiffness would be much lower than that of the transducer, and it would therefore exert no force. Certain other configurations of neoplastic tissue (e.g. a "capsule" firmly attached to the muscle or tendon at both ends and enclosing the transducer) might affect the measurement, depending on its stiffness compared to that of the enclosed muscle or tendon.

Fabrication

The base of the transducer frame (see Fig. 1) was laser-cut from Type 304 stainless steel (ss: HDE Systems, Sunnyvale, Calif.) and finished by hand. A removable cross-tube was made of 23 ga ss tubing, and bushings to support it were cut from 19 ga ss tubing and spot-welded to the base. A length of slit 30 ga ss tubing was bonded to the inner edges of the frame that the muscle or tendon would press on, to protect them from erosion.

U-shaped silicon micro strain gauges (Type P05-02-500) were selected for their high output and small size. Transducer frames were sandblasted to improve adhesion, the gauges were affixed with Epoxylite adhesive (6203FF: Epoxylite Corp., Irvine, Calif.), and clamped to the beams until set. Solder pads were affixed with Epoxylite, and the assemblies were heat cured (Psitronics Inc., Simi Valley, Calif.).

The gauges and surface wiring received an acrylic coating. Output leads were made from Bioflex AS-631, Teflon insulated, 40 ga, 10 strand, Type 316 ss wire (Cooner Wire Co., Chatsworth, Calif.), to which a silastic strain-relief tube was bonded. The lead assembly was soldered to, and potted with the pads. A 10 μ coating of Parylene-C was applied (Viking Technology Inc., San Jose, Calif.). A completed tranducer is shown in Fig. 2.

Static tests

We clamped the free side of the transducer frame (the side with the tie-down holes—see Fig. 1) so that the frame was horizontal, and repeatedly suspended and removed weights (calculated to bend the beams to the design limit) from the wire-lead side of the frame. No hysteresis was measurable in the transducer output. We then measured transducer sensitivity in a way that approximated its implanted configuration by fixing one end of a thread to a stand, passing it through the transducer, and hanging weights from the free end, in a temperature-controlled enclosure.

We calibrated each transducer with the thread in 5 positions: the thread parallel to the beams and bisecting the cross-tube represented a well-installed transducer with the eye neither elevated nor depressed; the thread at an extreme end of the cross-tube and parallel to the beams represented a well-installed tranducer with the eye in (unrealistically) extreme up-gaze or down-gaze; the thread running from one corner of the transducer aperture to the diagonally-opposite corner represented an extreme case of poor installation (see insets in Fig. 3). For each thread position weights were increased from 0 to 80 g, and then decreased back to 0 g. Representative static calibrations are shown in Fig. 3.

The four transducers we built had load sensitivities that were practically indistinguishable up to 40 g [Fig. 3(A)], showing that relevant aspects of fabrication were under good control.

With the eye in primary position, muscle force is uniformly distributed across the width of the muscle or tendon; in any cross-section the *centroid*, or effective point of application of this distributed force, is at the center. The test thread may be taken to represent a line connecting the centroids. As the eye rotates out of the "plane" of a muscle (e.g. a vertical rotation in the case of a horizontal muscle), the distribution of force across the width of the muscle or tendon becomes non-uniform, and the centroid line moves toward the stretched edge of the muscle. Centroid movement has been calculated to be ± 1.0 mm over a $\pm 30°$ field of gaze (Miller & Robinson, 1984). Figure 3(B) shows the effect of moving the test thread ± 2.5 mm. The effect of centroid displacement was small, almost unmeasurable up to 40 g. This helps ensure that force measurements are accurate for eye positions out of the plane of the measured muscle.

If the muscle were not parallel to the beams its dihedral angle with the cross-tube would be reduced, and load sensitivity decreased. Figure 3(C), which shows this effect for the extreme case in which the transducer was turned 45° out of alignment, shows that correct alignment is important. Accordingly, prior to implantation, we modified the gauges by drilling two small holes in the side of the frame opposite to the wire leads. During implantation, we used a non-absorbable suture to lightly

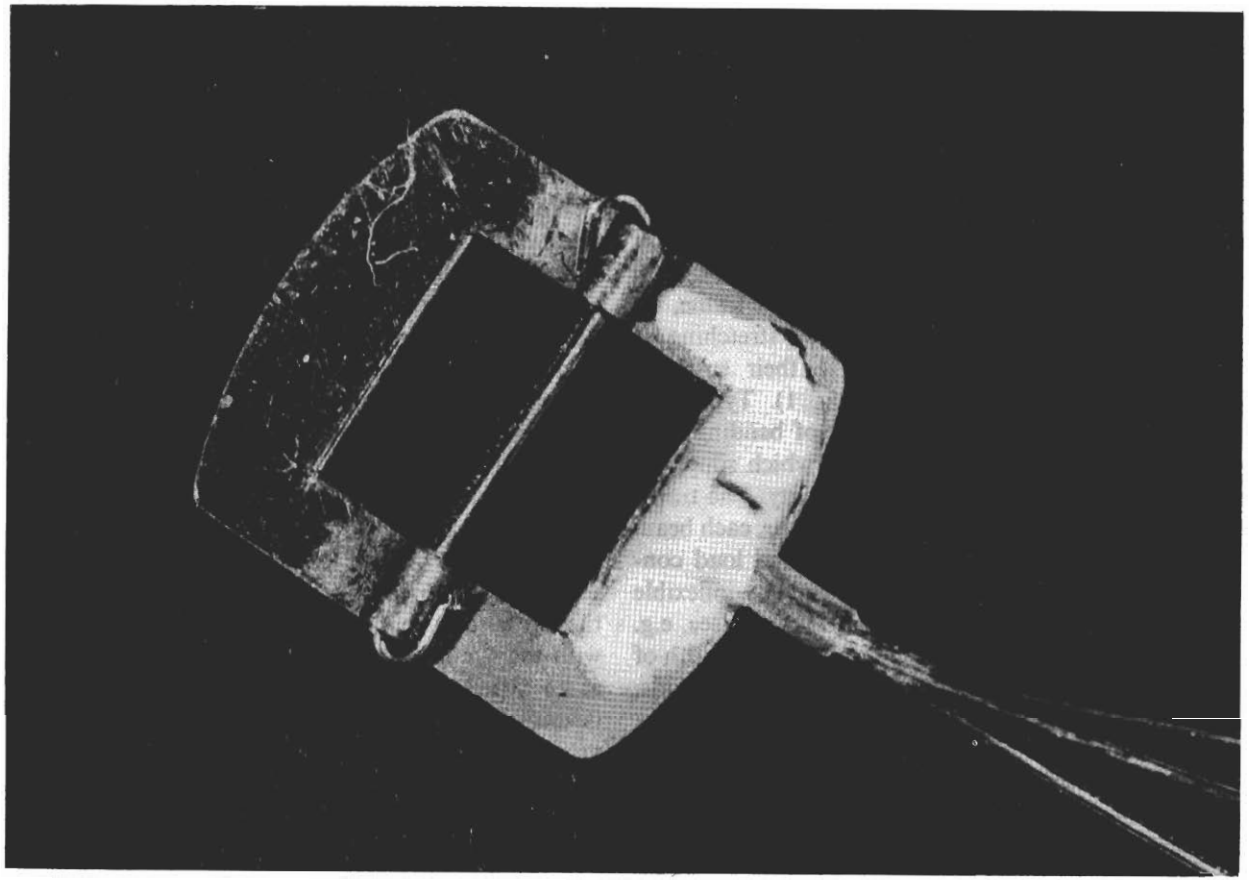

FIGURE 2. Transducer photograph. The device shown is finished and assembled, except for drilling the tie-down holes. The locking wire, shown inserted through the cross-tube, is normally installed after the device is attached to the muscle.

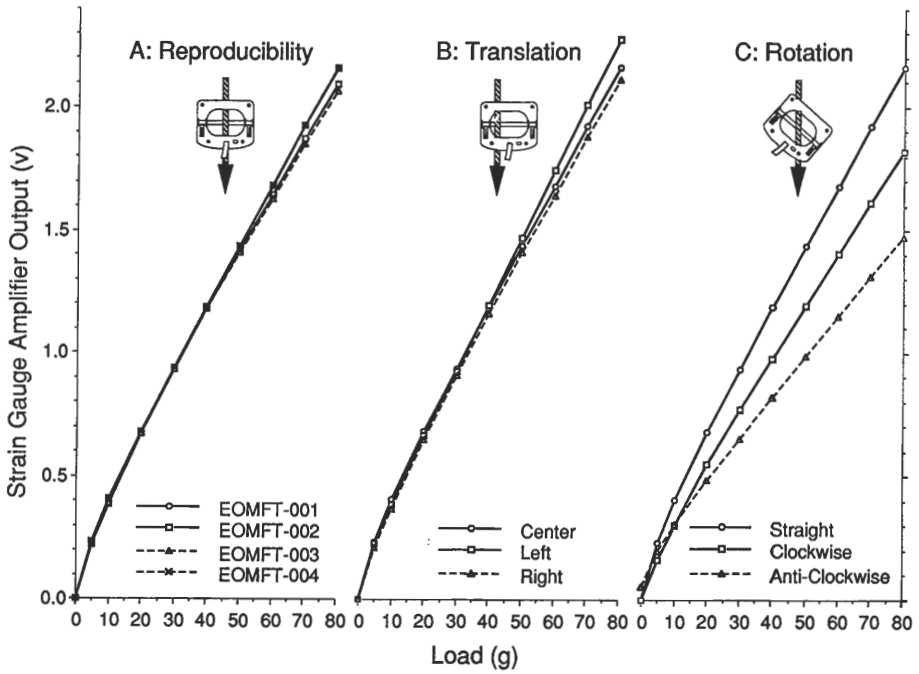

FIGURE 3. Static bench tests. (A) Reproducibility—the thread representing a muscle was parallel to and midway between beams (see inset). Measurements are shown for all four devices fabricated (data for EOMFT-001 and EOMFT-004 cannot be distinguished). (B) Translation—thread was parallel to beams and at center, extreme left (inset), and extreme right ends of cross-tube (EOMFT-004). (C) Rotation—thread passed from corner of transducer aperture to diagonally opposite corner, with transducer rotated clockwise (inset) or anti-clockwise, compared to normal, straight alignment (EOMFT-004).

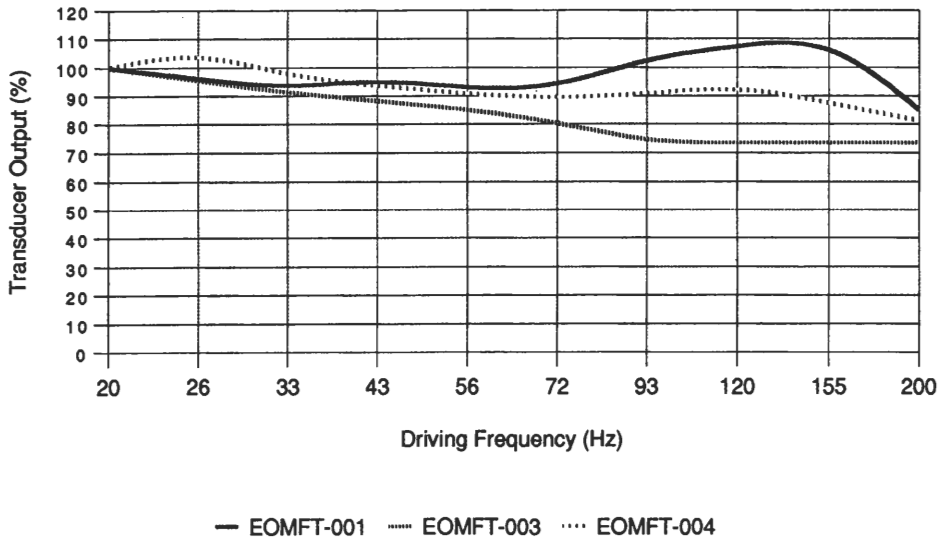

FIGURE 4. Frequency–response. The two unused transducers (EOMFT-001 and EOMFT-003) and the one still operating when excised (EOMFT-004) were tested with sinusoidal force inputs, as described in the text.

bind a bundle of muscle fibers to the frame, fixing the transducer's orientation (see Fig. 5).

Dynamic tests

Eye position signals have little energy over 40 Hz, and velocity signals have little energy over 74 Hz (Bahill, Brockenbrough & Troost, 1981). EOM force signals must have energy at higher frequencies, although we do not know their bandwidth. We measured transducer frequency–response between 20 and 200 Hz, the limits of our test apparatus.

The frequency–response test apparatus consisted of a low frequency audio driver with its exposed voice coil ridigly coupled to a thin steel rod, which passed through a linear position transducer, carrying the transducer's core. To the free end of the rod we attached a helical spring (stiffness = 50 g/0.1 in.), the other end of which was attached to a string fixed to the test frame. The EOM transducer under test was connected to an amplifier and mounted on the string, in which we then produced sinusoidally-varying tensions up to about 50 g. Outputs of the amplifier and linear position transducer were displayed on an oscilloscope. This measurement reflected the dynamics of the transducer under test, but also the dynamics of the spring and thread, and so only placed a worst-case limit on the transducer's frequency–response.

Frequency–response data are shown in Fig. 4. The surviving implant (tested after excision), and two devices that were not implanted, were all similarly flat from 20 to 200 Hz, the limits of testing.

Transducer implantation

All research conformed to the ARVO Resolution on the Use of Animals in Research. Surgery was performed under aseptic conditions, general anesthesia was induced with i.m. ketamine and i.v. pentobarbital, and analgesics and antibiotics were administered post-surgically, under supervision of a veterinarian.

The subject was an adult male *Maccaca fascicularis*. Prior to transducer implantation, a head restraint and scleral search coil (Robinson, 1963) were implanted. The coil was implanted in the left eye using the method of Judge, Richmond and Chu (1980), except that we sutured it to the sclera to prevent slip. When recovered, the animal was trained to fixate light spots for juice reward. During training, the search coil failed and had to be replaced. When training was complete a force transducer was implanted on the left LR, and 4.5 months later a second one was implanted on the left MR.

Force transducer implantation was straightforward. Following a 360° limbal peritomy, a rectus muscle was exposed through blunt dissection. Intermuscular membrane was pierced with a scissors at superior and inferior

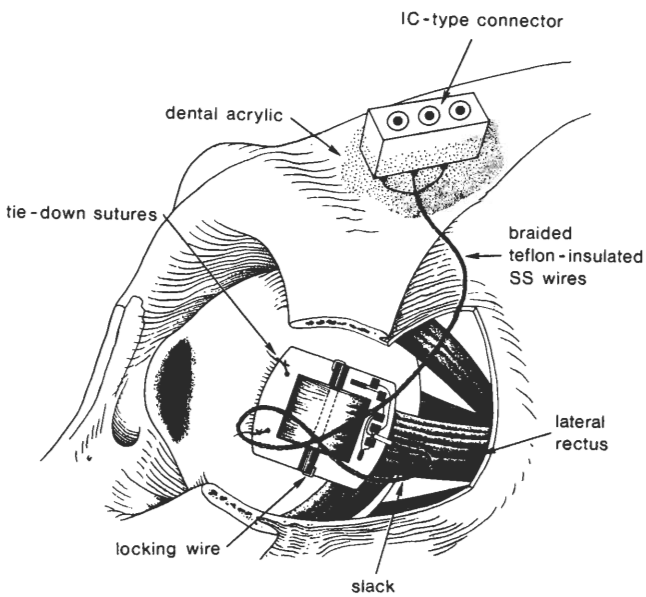

FIGURE 5. Implantation. The appearance of a transducer implanted on LR is shown in a drawing based on an X-ray image taken in lateral view, with the eye in primary position.

margins of the muscle, 5 mm posterior to the insertion. The transducer, with cross-tube removed, was placed face-up on the muscle with the leads extending posteriorly. With the muscle tented up through the center of the transducer frame on a muscle hook, the cross-tube and its locking wire were installed. To prevent the transducer from rotating, its anterior corners were sutured to the muscle with non-absorbable sutures. The signal leads were led posteriorly between the sclera and Tenon's capsule, looped back, and led out of the lateral (for LR) or superonasal (for MR) orbit under the skin. The globe was rotated to assure that the leads were not restricting motion. A hollow trocar carried the leads under the brow and scalp to exit at the edge of an acrylic cap, where a connector was mounted. Tenon's capsule and conjunctiva were smoothed back into position, and sutured to the limbal area with absorbable 7–0 chromic collagen sutures. The area of implantation was irrigated with 0.5 ml of injectable dexamethasone, 3 mg/ml, to minimize early scarring. A combination steroid-antibiotic ointment was placed on the eye. The installed transducers were visualized by conventional X-rays, from which Fig. 5 was drawn.

Post-mortem examination and measurements

We maintained the preparation until the LR transducer failed, 9 months after implantation. Failure was apparent as a change in the resistance of one silicon element from about 450 to several MΩ. The animal was sacrificed with an overdose of i.v. pentobarbitol, and both transducers excised, along with the muscles and the eye. Transducers and leads were found to be uniformly covered by a thin, tightly adherent connective tissue coat; apart from this, there was no evidence of foreign body reaction. No adhesions or scar tissue were found. Muscle and sclera in the vicinity of the transducer appeared normal, in particular, there was no evidence of abrasion or thinning of the sclera.

We determined that the upper silicon element of the LR transducer had failed. Microscopic examination revealed a cut in the Parylene-C coating on the bushing adjacent to the upper element, and separation of the coating from the substrate in that region. The coating appeared to have been damaged during installation of the locking wire.

Other instrumentation

Strain gauge amplifiers. We built strain gauge amplifiers, each based on an unbalanced Wheatstone bridge followed by a high-quality d.c. amplifier with calibrated gain and offset controls. The output of an unbalanced Wheatstone bridge is a linear function of strain gauge signal for our case, in which two active gauges, having equal and opposite strains, form two arms of the bridge.

Eye position measurement. The scleral search coil signal was processed by a lock-in amplifier (Princeton Applied Research, Model 129) followed by a custom-built amplifier, providing gain and offset controls. We adjusted its filter characteristics, and those of the strain gauge amplifiers, so that the response to step changes of eye position (simulated electronically by switching an eye coil tilted in the magnetic field) and step changes of muscle force (simulated with step changes of resistance) were synchronized to better than 0.15 msec at all points.

Computer control and stimulus presentation. Experiments were run on a Masscomp MC-5500 lab computer, controlled with custom software designed to provide high-level-language control of experiments requiring synchronous sampling and stimulus generation at kHz rates. The monkey, in an otherwise dark chamber, faced a display consisting of 25 red 0.125 in dia LEDs, arrayed at 10° intervals over a ±20° field. Each msec, we sampled eye position (H and V) and muscle force (LR and MR), detected saccades by a velocity criterion, updated the monkey's LED target display, and updated the experimenter's monitor, which showed the target board, the monkey's eye position, and effective eye position windows. The monkey was rewarded and targets were sequenced automatically.

Data collection

Each experimental session began with calibration of the search coil system. Targets were lit in random order. The experimenter judged when the monkey was on target by viewing a monitor that showed target and fixation positions, and pressed a button to record eye positions, reward the monkey, and select the next target. The set of calibration targets was presented several times, and the mean fixation values for each target were stored, to be used to correct eye position signals during experimental trials.

Following calibration, the program took complete control of the experiment. Each experimental trial began with presentation of a random target. The monkey was required to initiate a saccade that ended inside a neighborhood proportional to the distance of the lit target LED. This encouraged single, accurate saccades of all sizes and directions. The monkey then had to fixate within 1.5° of the target to earn the first reward. Maintaining fixation for an additional random period between 1.5 and 3.0 sec earned the second reward. This encouraged accurate, quiescent fixation of each target. Following each successful trial (both rewards received), the target was extinguished and the next randomly selected target was immediately presented. Following each unsuccessful trial, a 4 sec time-out was interposed before the next target was presented.

All experimental events were timed, and all samples were acquired with 1 msec temporal resolution. Position and force data were sampled with 12 bit precision.

Data analysis

Data was analyzed automatically using Unix* utilities and custom programs written mostly in C. Calibration of eye position signals has already been described. Calibration of muscle force signals using data collected (as described above) before transducer implantation and after removal is straightforward in principle. However,

*Trademark of AT&T.

in the present case, modifications to the amplifiers during the experiment, and probable errors in experimental procedure, left us with unreliable calibrations. Therefore, we report muscle forces as percentages of the total range for a data collection session, during which 1500 saccades were recorded. This range was fairly stable across sessions ($\sigma/\bar{x} = 6\%$, $n = 4$). Thus, a force of 0% was assigned to a muscle when it was in the role of antagonist, maximally inhibited during a large saccade, and a force of 100% when a muscle was agonist, maximally excited during a large saccade. As will be seen, excitatory and inhibitory peaks occurred near the ends of horizontal saccades (Fig. 9). Thus, a force of 0% probably corresponded to near 0 g contractile (developed) force; elastic and viscous muscle forces would generally be greater than zero. Similarly, a force of 100% probably corresponded to near maximal saccadic contractile force; elastic force would be submaximal, and viscous force would be negative (i.e. would reduce total tension).

Saccadic variations in position and force signals were detected offline using a pattern-sensitive criterion that was relatively insensitive to variations in noise levels (only position signals had significant noise). The saccade detection program found a beginning of a saccade only if it was followed within 100 msec by an end of saccade, which in turn was followed after 100–150 msec by a post-saccadic steady state. The beginning of the saccade was located at the force or position sample that was at the start of a sufficiently rapid acceleration. For eye position channels, the time series of threshold velocities was: 20, 40, 60, 80, 100, 120 and 140 deg/sec, computed as differences of successive 1 msec samples. For muscle force channels, the sequence of threshold rates of change was: 80, 160, 240, 320 and 400 %/sec. The end of the saccade was located at the sample where the signal reversed direction (the excitatory or inhibitory peak of force signals, or the overshoot of position signals) or first assumed a steady value (the end of normal position saccades). We verified the performance of the saccade detector by comparing it to visual judgments of the experimenter.

We concentrated our analyses on a group of four sessions near the end of the 9 month period of study, in which all of 25 fixation targets were presented. These data are the basis of the quantitative results that follow.

RESULTS

Tonic forces over the field of gaze

Muscle forces measured 200 msec after the end of a saccade that brought the monkey's eye into the "fixation window" surrounding a target LED (see *Methods/Data collection*) were taken as the tonic forces associated with fixation of that position. The fixation data from 4 sessions in which all 25 targets were presented are summarized in Fig. 6. Figure 6(A) shows LR tonic fixation force over the $\pm 20 \times \pm 20°$ field of gaze. LR force varied over a 25% range, with primary position force being 31%. LR force increased in abduction in a roughly linear fashion, although slope tended to increase in abduction. There appeared to be some dependence of force on vertical eye position out of the LR field of action (i.e. in adduction), such that smaller forces were measured in downgaze and extreme upgaze. Tonic LR tension remained well above 0% at all measured fixation positions.

MR tonic fixation force [Fig. 6(B)] increased in adduction, covering a larger range and showing greater nonlinearities than LR force. MR fixation force varied over a 42% range, with primary position force being 35%. Slope was clearly increasing with large forces, and dependence of force on vertical eye position out of the MR field of action had the same pattern as with LR, but was more marked. MR fixation forces covered a larger fraction of the total force range than did LR fixation forces.

The data of Fig. 6 are re-plotted in Fig. 7 to show the reciprocal relationship of LR and MR forces, and the

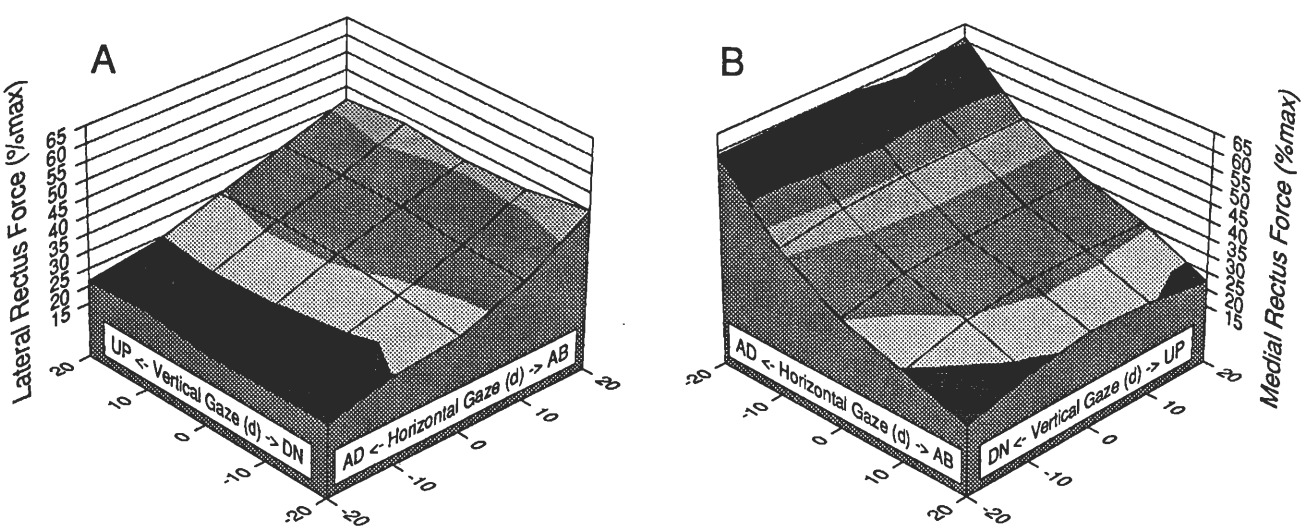

FIGURE 6. Fixation forces. Force surfaces and iso-force contours are shown for fixations over a $\pm 20 \times \pm 20°$ field. Gaze angles are in deg arc (abduction and upgaze are +). Muscle forces are given as percent of the maximum force measured in the data collection session (see text). (A) Lateral rectus forces. (B) Medial rectus forces.

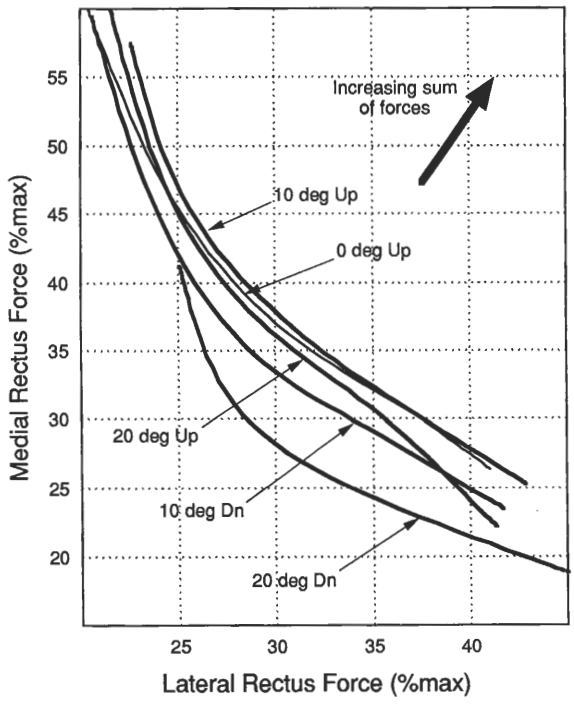

FIGURE 7. Reciprocal innervation is demonstrated by plotting MR force against LR force, over the range of horizontal eye positions, with vertical eye position as the parameter. The wide arrow indicates the gradient, or direction of most rapid increase, of the sum of LR and MR forces.

dependence of this relationship on vertical eye position. Tensions were largest 10° in elevation, falling at greater and lesser elevations to minimal values at 20° depression.

Slow changes in muscle force

Figure 8 shows fixation forces, first recorded 15 days after implantation of the LR transducer and continuing for 20 weeks (at which time the MR transducer was implanted). Most apparent in 20° abduction was an exponential decrease in force with a time constant of about 10 days. The signal became fairly stable about a month after implantation, although downward drift continued at the highest force levels in extreme abduction.

Horizontal saccades

Representative horizontal saccades are shown in Fig. 9. The 4 saccades shown all began within about 1° of primary position, and had minimal vertical components.

Figure 9(A) shows an 18° abducting saccade. Tension in the agonist LR rose rapidly from a pre-saccadic level of 29% of session maximum to a peak of 75% of maximum (right ordinate), and then dropped, first at a rate similar to its rise, and then more slowly, to a post-saccadic level of 41%. Tension in the antagonist MR dropped rapidly from a pre-saccadic level of 37% to an inhibitory peak of 15%, then recovered, first at a rate comparable to its drop and then more slowly, finally settling to a post-saccadic level of 27%. A smaller, 10° abducting saccade is shown in Fig. 9(B). Compared to the saccade of Fig. 9(A), muscle tensions had smaller peaks, and settled to post-saccadic values that were closer to pre-saccadic values, but were otherwise similar to those of Fig. 9(A). Skipping to Fig. 9(D), we show a 10° adducting saccade. Excitatory and inhibitory force peaks, and differences between pre-saccadic and post-saccadic resting tensions, were larger than those in the 10° abducting saccade of Fig. 9(B). Finally, the 16° adducting saccade shown in Fig. 9(C) was in most respects a scaled-up version of the 10° adducting saccade, except that the inhibitional peak in the antagonist LR appeared to be reaching saturation. It is possible that minimum contractile force was approached as total LR force dropped below 10%, with the non-zero total force being due to elastic, and possibly viscous, forces.

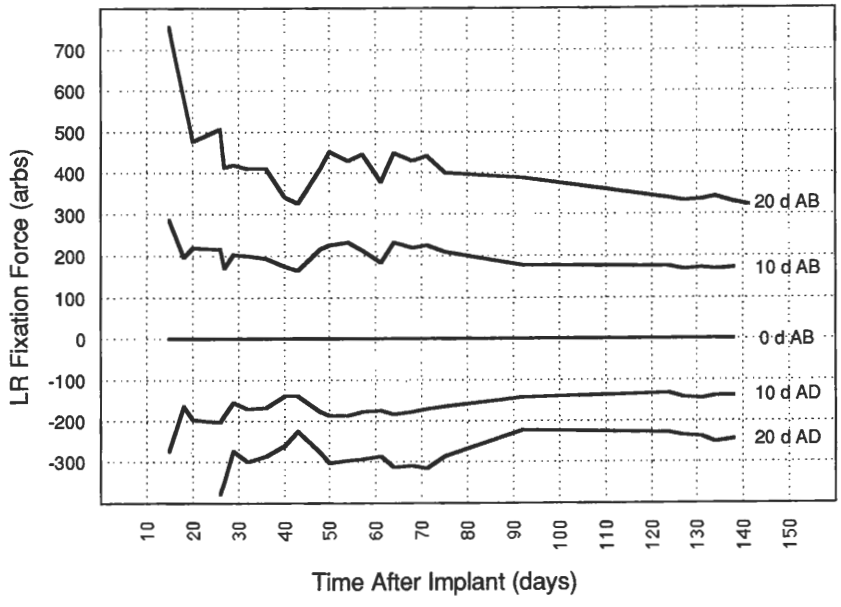

FIGURE 8. Stability. LR fixation force at each horizontal fixation angle (relative to that for the median plane, and averaged over vertical angles) is shown as a function of time after implant, beginning at 15 days and ending just before the MR transducer was implanted. To allow comparison across days, force is expressed in fixed, albeit arbitrary, units.

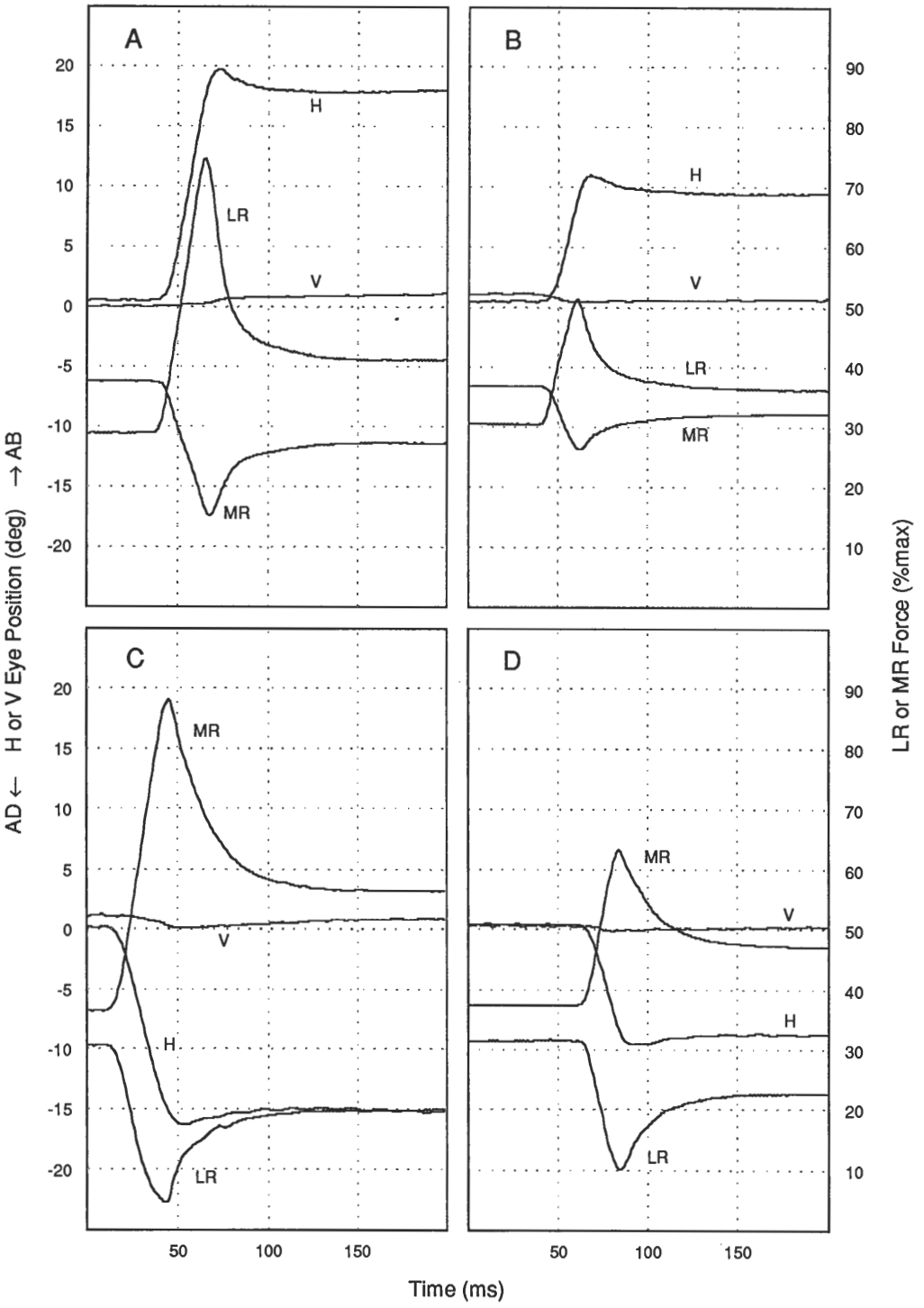

FIGURE 9. Horizontal saccades. Each panel shows a 200 msec duration record of horizontal (H) and vertical (V) eye position (left ordinate) and lateral rectus (LR) and medical rectus (MR) force (right ordinate) for a horizontal saccade from primary position. Positions are given in deg arc (abduction is +), and forces as percent of the maximum force measured in the data collection session. (A) Large (18°) abducting saccade. (B) Small (10°) abducting saccade. (C) Large (16°) adducting saccade. (D) Small (10°) adducting saccade.

The saccades of Fig. 9, and all other horizontal saccades we observed, had agonist and antagonist tensions with similar time–courses, that is, tensions were similar within a scale factor. Both excitatory and inhibitory force peaks were generally symmetrical about their extrema [apart from presumed saturation effects as in Fig. 9(C)]. Despite the complication of centripetal glissades (Weber & Daroff, 1972; Bahill, Clark & Stark, 1975b) in most horizontal saccades, it was clear that eye position settled well before muscle force, which did not reach equilibrium until roughly 100 msec after its peak in agonist and antagonist. None of the antagonist traces in Fig. 9 show any sign of active braking by the antagonist at the end of saccades; we never saw antagonist force rise above its post-saccadic equilibrium value, following its inhibitory peak. Nor did we ever see a transient increase in antagonist tension near the beginning of a saccade.

Vertical saccades

Representative vertical saccades are shown in Fig. 10. In Fig. 10(A) the eye makes a downward saccade of 20° through primary position. We were surprised to find a substantial transient reduction in MR tension (10%), and a smaller, more variable reduction in LR tension during such saccades. The dip in MR tension was seen in upward vertical saccades as well [Fig. 10(B)], and at all horizontal gaze angles, except in extreme adduction, where a dip near the beginning of an upward or downward saccade was usually followed by a peak near the end. A clear example of this biphasic force profile is shown in Fig. 10(C). As the eye moved into extreme abduction, the dip in LR tension became a peak [Fig. 10(D)], again for both upward and downward saccades.

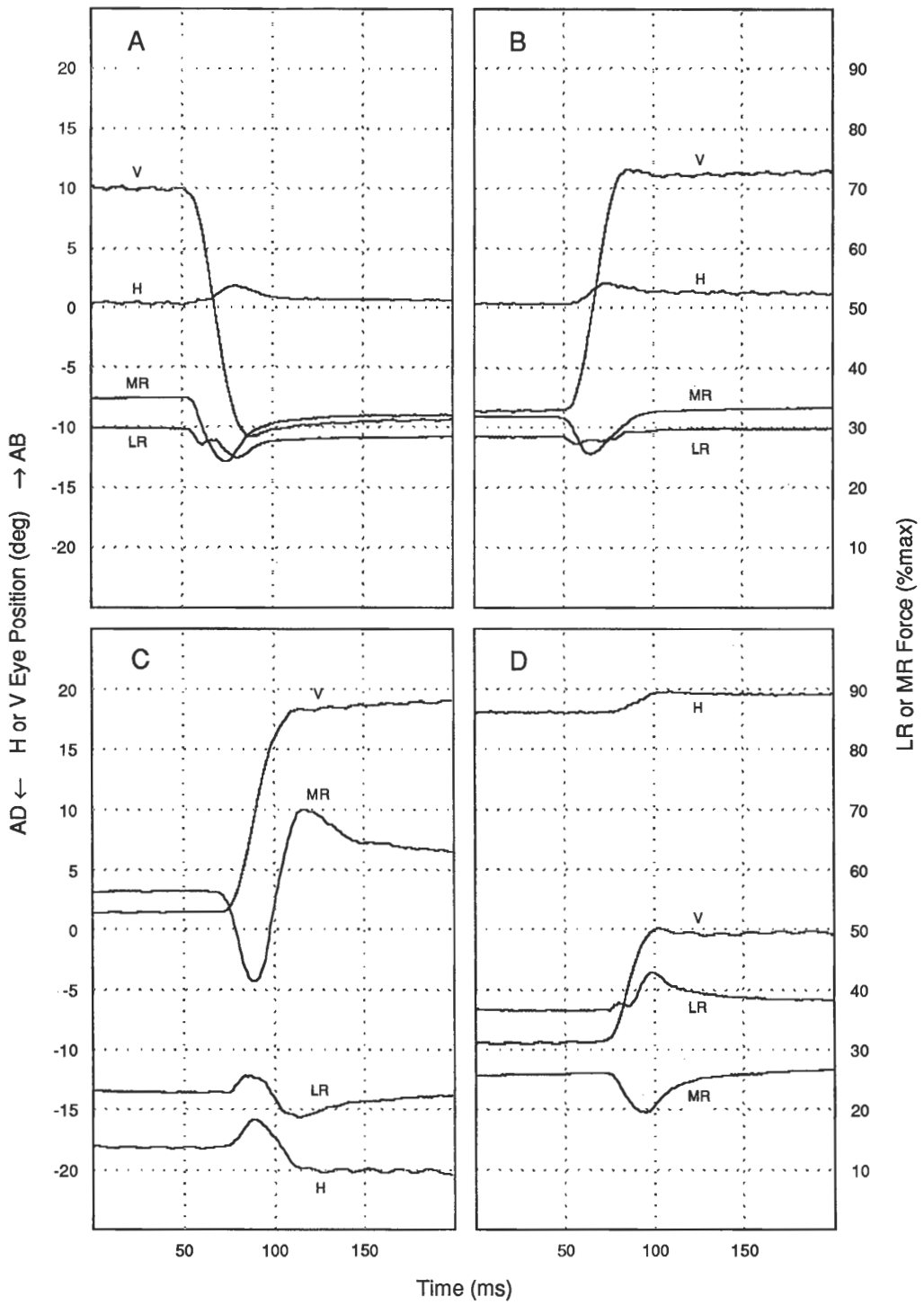

FIGURE 10. Vertical saccades. Each panel shows a 200 msec duration record of horizontal (H) and vertical (V) eye position (left ordinate) and lateral rectus (LR) and medial rectus (MR) force (right ordinate) for a vertical saccade. Positions are given in deg arc (abduction is +), and forces as percent of the maximum force measured in the data collection session (see text). (A) 20° downward saccade, about primary position. (B) 20° upward saccade, about primary position. (C) 17° upward saccade from 13° adduction. (D) 9° upward saccade from 18° abduction.

It is also apparent in Fig. 10 that horizontal rectus resting tension was a function of vertical eye position (see *Results/Tonic forces over the field of gaze*).

Pulse timing in antagonistic muscles

At the temporal resolution of Fig. 9, it appears that the onsets of excitatory and inhibitory tension pulses associated with horizontal saccades were simultaneous in agonist and antagonist muscles. However, with greater temporal resolution, this is seen not to have been the case (Fig. 11). We analyzed all saccades having horizontal components $>8°$ and vertical components $<4°$. By eliminating small horizontal saccades we avoided the uncertainties of locating the onsets of small pulses. By eliminating saccades with large vertical components we minimized effects of cross-coupling (Fig. 10). The resulting sample of saccades had a mean (absolute) horizontal size of 13.4° and a mean (absolute) vertical size of 1.8°. We located pulse onsets in the force channels, and movement onsets in the horizontal position channel automatically, using the pattern matching algorithm described in *Methods*. Excitatory LR pulse onset led eye movement by 2.6 msec ($\sigma = 1.4$, $n = 158$), while inhibitory MR pulse onset led eye movement by 1.0 msec ($\sigma = 1.7$, $n = 158$). Excitatory MR pulse onset led eye movement by 4.1 msec ($\sigma = 1.5$, $n = 93$), while inhibitory LR pulse onset led eye movement by 3.0 msec ($\sigma = 1.5$, $n = 93$). This means that excitatory LR pulses led inhibitory MR pulses by 1.6 msec ($\sigma = 1.2$, $n = 158$), and excitatory MR pulses led inhibitory LR pulse onsets by 1.1 msec ($\sigma = 0.8$, $n = 93$).

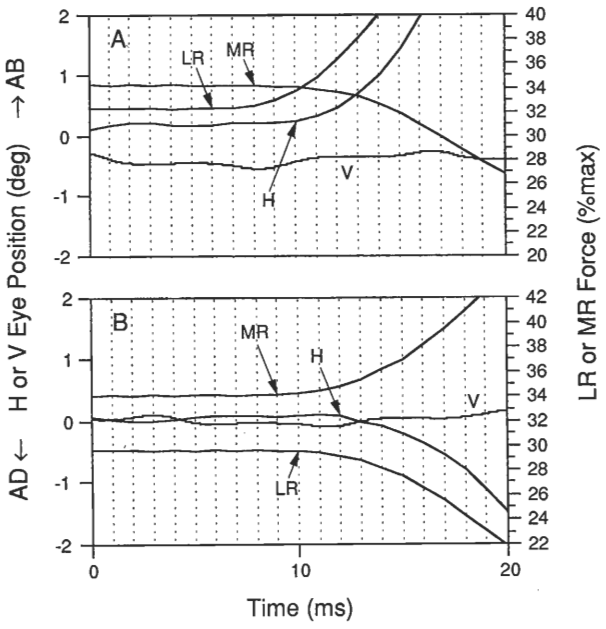

FIGURE 11. Horizontal saccades at high temporal resolution. Each panel shows a 20 msec record of horizontal (H) and vertical (V) eye position (left ordinate) and lateral rectus (LR) and medial rectus (MR) force (right ordinate) for a horizontal saccade from primary position. Positions are given in deg arc (abduction is +), and forces as percent of the maximum force measured in the data collection session. Vertical grid lines mark 1 msec samples. Arrows point to the sample at which the saccade detector located the beginning of the saccade. (A) 20° abducting saccade. The agonist LR tension pulse (LR) was detected first, followed two samples (i.e. 2 msec) later by the inhibitory antagonist MR pulse (MR), followed two samples later by horizontal eye movement (H). The vertical eye position channel (V) showed only 60 Hz noise. (B) 8° adducting saccade. Saccadic activity was first detected in agonist MR, then 1 msec later in antagonist LR, and then 1 msec later in the horizontal component of eye position.

DISCUSSION

Transducer

We described the design and fabrication of the first extraocular muscle force transducer suitable for chronic study of the eye's 3-dimensional mechanics. Although fabrication was complex, the resulting devices had well-controlled characteristics. Output of a properly installed device was close to a linear function of total muscle force summed across the width of the tendon, and had insignificant hysteresis and low noise. Frequency response was fairly flat up to the 200 Hz limit of testing. We believe that the frequency–response was actually flatter than Fig. 4 indicates, but that this was obscured by resonances and other limitations of the testing apparatus. Of the two transducers implanted, one functioned *in vivo* for 9 months and then failed, and the other was functional when it was excised 5 months after implantation. The monkey's eye healed well from both implantation surgeries, and both devices were tolerated without inflammation or damage to orbital structures.

Several areas for device improvement are apparent. Since the transducer operates by deforming (slightly) under muscle tension, one worries that it may deform in contact with the orbital wall, or that as the muscle wraps around the globe in extreme gaze, the anterior edge of the transducer frame might be lifted out of contact with the muscle. Finally, as we noted in *Results*, implantation of the prototype devices may have contributed to increased orbital stiffness in extreme (abducting) gaze. All of these worries would be assuaged by making the device smaller. A redesigned transducer is currently being built, with overall dimensions 6×5.5 mm.

Although transducer output became relatively stable a month after implantation, output continued to decrease slowly with time (Fig. 8). The tie-down sutures and the connective tissue sheath that grew around the transducer and muscle made it unlikely that this was due to rotation [see Fig. 3(C)] or other movement of the transducer. The slow decrease might have reflected true muscle adaptation, growth of a stiff connective tissue "capsule" around the transducer (see *Methods*), or decay of intrinsic transducer sensitivity. No capsule-like growth was apparent when the transducers were excised, although not having made specific mechanical tests, it is hard to eliminate this possibility. Reducing the size of the transducer, and so the length of included tendon or muscle, would make this less of a worry in the future. The intrinsic sensitivity of the transducer could have decayed through moisture penetration or weakening of the bond between the silicon strain gauges and the transducer frame. The latter could be minimized by sacrificing device sensitivity to reduce the maximum strain applied to the gauge.

Tonic forces over the field of gaze

Modeling of the static mechanics of the orbit has proceeded with difficulty, due in part to the paucity of EOM force data (Miller & Robinson, 1984). The pioneering work of Collins, Scott and O'Meara (1969) and Robinson, O'Meara, Scott and Collins (1969) in humans made it possible to construct the first plausible static model (Robinson, 1975), although the limitations of these data have always been recognized: only abnormal horizontal rectus muscles were measured. Indirect measurements of normal human horizontal recti have since been obtained (Collins, Carlson, Scott & Jampolsky, 1981), but significant gaps and uncertainties remain concerning muscle forces in normal, intact eyes. Direct measurements of muscle forces over a full field of gaze, and reliable primary-position measurements, for instance, are not available, despite their central importance in static modeling.

We have approached this problem by developing human and monkey models of ocular statics in parallel (Miller & Robinson, 1984; Miller & Robins, 1987; Miller, 1989). We sought to begin collecting the needed monkey data by measuring fixation forces over a substantial field of gaze for both horizontal recti. This first attempt was only partly successful since we were not able to express our force measurements in absolute terms (see *Methods*). Nevertheless, the fixation data collected are of interest.

The fixation force surfaces of Fig. 6 show, not surprisingly, that horizontal rectus forces were mainly a function of horizontal gaze angle. However, there is a slight suggestion in our LR data [Fig. 6(A)], and a strong suggestion in our MR data [Fig. 6(B)], that horizontal rectus force was also a function of vertical eye position. This is seen in the curvature of the contour lines of Fig. 6, and in the ordering of the curves for different vertical gaze positions in Fig. 7. From Fig. 6(B), for example, it can be seen that MR forces at given straight and abducted horizontal gaze angles, were maximal 5 or 10° in elevation, and minimal in extreme depression. From Fig. 7 it can be seen that the sum of LR and MR forces was maximal at 10° elevation, and minimal at 20° depression. This may have been a consequence of monkey orbital geometry. Miller and Robins (1987, Table 1) found that rectus muscle origins are about 6 mm below the eye's center of rotation, that is, the monkey orbit is pitched upwards about 16°. There might, then, be a tendency for horizontal recti to be maximally stretched at 16° elevation, depending on details of the orbital fascia (Miller, 1989; Miller, Demer & Rosenbaum, 1990). A geometrical explanation of this sort would attribute the curvature of contours in Fig. 6 to changes in elastic force only. This would allow contractile force, and so innervation, to be constant for a given horizontal gaze angle. There is evidence that individual LR and MR motoneuron firing rates are independent of vertical eye position (Hepp & Henn, 1985), although these data do not take account of recruitment patterns.

MR forces rose more steeply in adduction than LR forces did in abduction. It is possible that the four orbital surgeries (see *Methods*) increased orbital stiffness in extreme adduction. An indication of this was that the animal had some difficulty accurately fixing targets requiring extreme adduction. But even if we suppose that the steep rise in MR force was partly artifactual, we can ask why this muscle was differentially affected. The MR is a short muscle (20 mm, including tendon) in monkey, and orbital geometry is such that it begins to lose tangency with the globe, at roughly 10–20° adduction, depending on details of the insertion and individual differences (Miller & Robins, 1987, Table 1). Thus, the steep rise in MR force at extreme adduction could be largely physiological, exacerbated perhaps by surgically induced scarring.

Single unit data from the abducens nucleus for 20° saccades has a primary time constant of 70–90 msec, accounting for about 40 spikes/sec change (Goldstein, 1983), and a much longer secondary time constant, accounting for about 15 spikes/sec (Goldstein, personal communication). To avoid intrusion of microsaccades, which would have introduced additional transients, we measured tonic forces 200 msec after the ends of saccades. This delay allows for the first decay time, but not for the second. We did not specifically address the issue of hysteresis, but its effects should be minimal in our mean data because we randomized the order of target presentations.

Slow changes in muscle force

It is known that chronically stretched (or shortened) skeletal muscles add (or subtract) sarcomeres (Tabary, Tabary, Tardieu, Tardieu & Goldspink, 1972; Williams & Goldspink, 1973), in order to optimize overlap of myofilaments, and so contractile force, in the operating range (Williams & Goldspink, 1978). Scott (1992) has recently demonstrated that sarcomere length in chronically stretched or shortened monkey horizontal recti is normalized within 2 months. Thus, the reductions in fixation forces we measured in the first month may reflect adaptation to the increase in muscle path length caused by the transducer. This increase ($\sim$0.25 mm) was quite small, however, and we tend to attribute most of this effect to reduction in orbital stiffness as surgical trauma resolved. The very slow reductions that continued to occur may indicate instability in the muscle force transducer itself (Fig. 8).

Horizontal saccades

The EOM force transducer responds to contractile, elastic and viscous muscle forces. As an agonist shortens, elastic force decreases and viscous force may become negative. As an antagonist lengthens, elastic force increases and viscous force is positive. Still, total force should be dominated by contractile force during a saccade, and we expect to see waveforms with the general shapes expected from the "pulse–slide–step" pattern of saccadic motoneuron firing (Goldstein, 1983; Goldstein & Robinson, 1986). This, indeed, was always the case (e.g. Fig. 9).

We found that agonist and antagonist waveforms were always similar, within a scale factor. Pfann, Miller and Keller (1991) show that this finding may be sufficient to reject such models of orbital dynamics as that of Lehman and Stark (1983), which predict highly asymmetric agonist and antagonist tension waveforms, and other features inconsistent with the present findings.

Evidence of active braking by the antagonist at the end of a saccade has been sought in EMG and motoneuron studies. Sometimes it is found (Sindermann, Geiselmann & Fischler, 1978; Van Gisbergen, Robinson & Gielen, 1981), and sometimes not (Goldstein, 1983). Our direct measurements seem to decide the matter: we have never seen antagonist muscle force do anything other than smoothly approach post-saccadic equilibrium. This was the case even for saccades like those shown in Fig. 9(A) and (B), which showed what has been called "dynamic overshoot", in reference to their presumed cause in control signal reversals (Bahill *et al.*, 1975a).

We also never saw a transient increase in antagonist force near the beginning of a horizontal saccade, as was reported by Collins *et al.* (1975) in strabismic humans. Such an increase might occur in viscous and elastic muscle forces if the globe began to rotate before the antagonist relaxed. It is possible that human eyes are different from monkey eyes in this respect.

Even with these very cursory discussions of orbital dynamics, the importance of muscle force data should be clear. Future dynamic modeling efforts should be supported by studies in which eye position, muscle tensions, and impulse rates of representative samples of motoneurons are measured.

Vertical saccades

We observed complex changes in horizontal muscle forces during vertical saccades. We are inclined to attribute the transient dips in tension, seen in MR in all horizontal gaze angles and in LR in all but abducted gaze (Fig. 10), to posterior globe translation (retraction) caused by superior rectus (SR) contraction during upward saccades and inferior rectus (IR) contraction during downward saccades. Transient peaks in horizontal rectus tension in adducted gaze [Fig. 10(C)] may be due to anterior globe translation caused by inferior oblique (IO) contraction during upward saccades, and superior oblique (SO) contraction during downward saccades. The LR peaks in abduction [Fig. 10(D)] remain puzzling.

Pulse timing in antagonistic muscles

Reversing the roles of LR and MR caused a shift of 2.7 msec in the tension–response times, such that the agonist always led. This may have been due to faster motor unit response at higher excitation. We found that eye movement lagged tension increase in agonist LR by 2.6 msec, and tension decrease in antagonist LR by 3.0 msec. Fuchs and Luschei (1970) found that eye movement lags abducens motoneuron excitatory pulse onset by 6.1 msec, and the abducens inhibitory pulse onset by 8.4 msec. Comparison of our data with those of Fuchs and Luschei (1970) suggests that the events between motoneuron firing and the appearance of muscle tension (motoneuron conduction, neuromuscular synaptic transmission, and EOM excitation–contraction coupling) consume 3.5 msec for LR excitation and 5.4 msec for LR inhibition (Fig. 12).

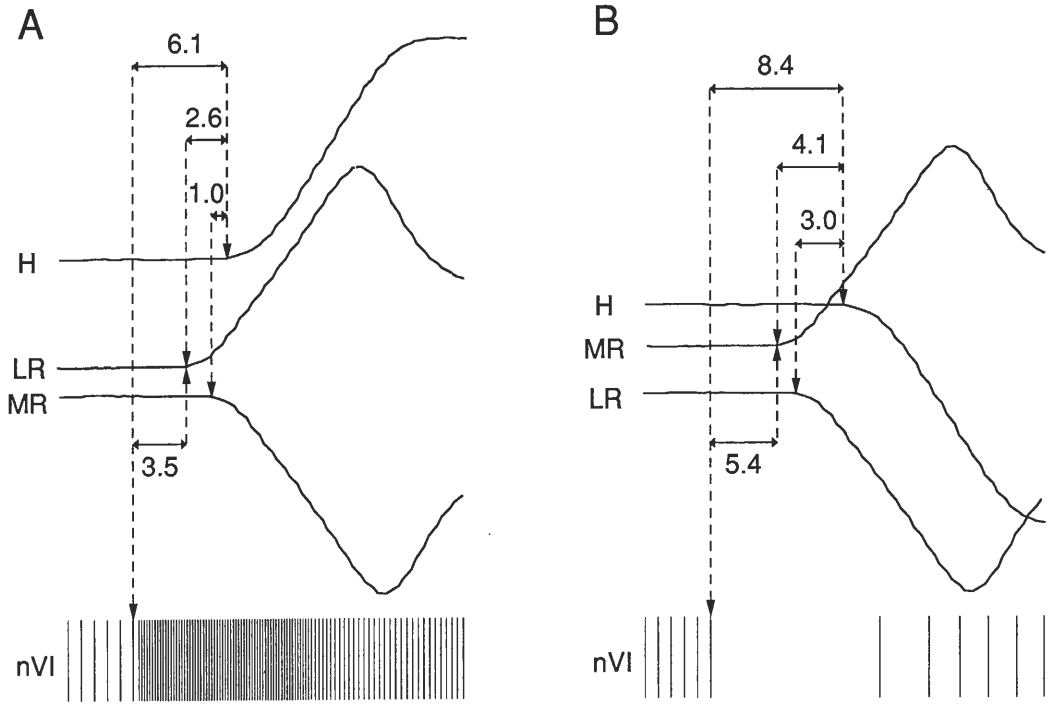

FIGURE 12. Beginning-of-saccade mean signal timing. This graphical summary shows the mean timing of onsets of muscle tension pulses (LR, MR; up = increase) and eye movement (H; up = abduction) as found in the present study, compared to the mean onset of saccade related changes in abducens motoneurons (nVI) as reported by Fuchs and Luschei (1970). Times are in msec. (A) Abducting saccade. (B) Adducting saccade.

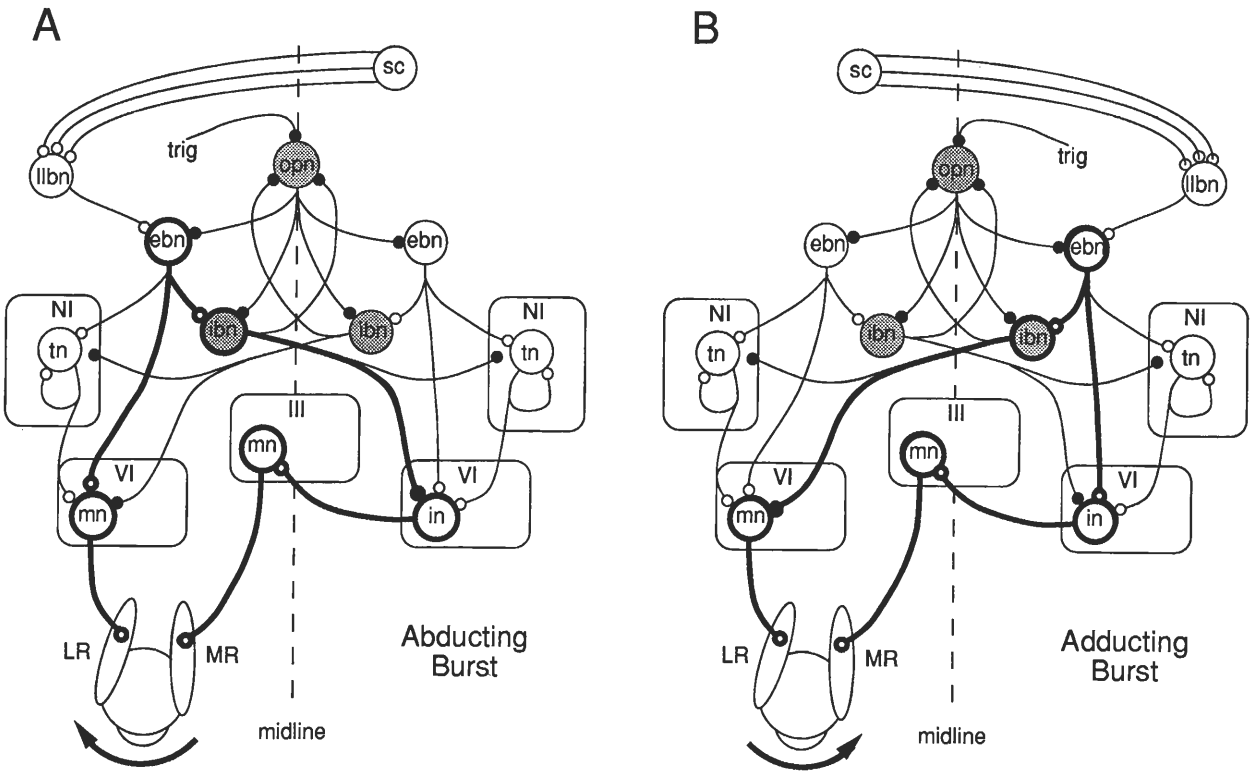

FIGURE 13. Saccadic burst neuroanatomy, adapted from Keller (1980), Robinson (1981) and Fuchs, Kaneko and Scudder (1985), as a plausible model of brainstem functional connectivity. Heavy outlines highlight the direct (burst) pathway, downstream from the point of divergence to LR and MR. Small open circles are excitatory synapses, and small solid circles are inhibitory synapses. (A) LR is agonist and MR is antagonist. The direct pathway to LR is shorter by 2 synapses than that to MR. (B) MR is agonist and LR is antagonist. The direct pathway to LR contains the same number of synapses as that to MR. (III, oculomotor nucleus; NI, neural integrator; VI, abducens nucleus; ebn, excitatory burst neuron; ibn, inhibitory burst neuron; in, internuclear neuron; llbn, long-lead burst neuron; mn, motoneuron; opn, omnipause neuron; sc, superior colliculus; tn, tonic neuron; trig, trigger signal).

A second—not incompatible—explanation is suggested by brainstem connectivity. Figure 13 is a model of the connectivity of brainstem neurons involved in horizontal saccades. In Fig. 13(A) we have highlighted the neurons involved in abducting saccades (LR agonist), from the excitatory burst neuron (ebn) to the muscles, and in Fig. 13(B) we have done the same for adducting saccades (MR agonist). Simply counting synapses reveals that for both LR and MR, the saccadic burst has one more synapse to traverse when the muscle is antagonist (3 for LR, 4 for MR) than when it is agonist (2 for LR, 3 for MR). Differences in conduction times should be considered in a more detailed analysis.

The mean time of onset of the decrease in antagonist tension might have been delayed by stretching. However, any such effect would have to be small, since otherwise we would expect the measured variability in force and position signal timing to result in at least an occasional increase in antagonist tension, which, as we have noted, was never seen. Thus, onsets of pulse increases and decreases in total muscle tension may be taken as reflecting changes in contractile tension in both agonist and antagonist, with elastic tension maintained at presaccadic values.

We found that the eye responded faster when abducting than adducting, to both agonist (difference of 1.5 msec) and antagonist pulses (difference of 2.0 msec). This may be related to the finding of Collewijn, Erkelens and Steinman (1988) that abducting saccades have larger size, higher peak velocity, and shorter duration than adducting saccades to a target of the same retinal eccentricity.

Future directions

The results we have reported should of course be refined and extended. Many other studies, not touched upon here, become possible with the extraocular muscle force transducer. The effects of stimulation and lesioning of the brain, and of pharmacologic manipulation of muscles, could be studied at higher resolution and with greater refinement than is possible with eye position measures. The empirical content of static and dynamic ocular models could be increased by testing them against muscle tension data. Agonist–antagonist cocontraction, undetectable in eye rotation data, would be apparent in muscle force signals.

Unlike the scleral search coil (Robinson, 1963), the extraocular muscle force transducer cannot be fabricated at one's lab bench. Several stages of fabrication are not economically practical for a small number of devices. Accordingly, we will undertake to supply these devices to interested investigators. Improved devices, scaled for monkey and for human eye muscles, are currently being fabricated.

REFERENCES

Bahill, A. T., Brockenbrough, A. & Troost, B. T. (1981). Variability and development of a normative data base for saccadic eye movements. *Investigative Ophthalmology and Visual Science, 21,* 116–125.

Bahill, A. T., Clark, M. R. & Stark, L. (1975a). Dynamic overshoot in saccadic eye movements is caused by neurological control signal reversals. *Experimental Neurology, 48,* 107–122.

Bahill, A. T., Clark, M. R. & Stark, L. (1975b). Glissades—eye movements generated by mismatched components of the saccadic motoneuronal control signal. *Mathematical Biosciences, 26,* 303–318.

Collewijn, H., Erkelens, C. J. & Steinman, R. M. (1988). Binocular co-ordination of human horizontal saccadic eye movements. *Journal of Physiology, 404,* 157–182.

Collins, C. C., O'Meara, D. & Scott, A. B. (1975). Muscle tension during unrestrained human eye movements. *Journal of Physiology, 245,* 351–369.

Collins, C. C., Scott, A. B. & O'Meara, D. M. (1969). Elements of the peripheral oculomotor apparatus. *American Journal of Optometry, 46,* 510–515.

Collins, C. C., Carlson, M. R., Scott, A. B. & Jampolsky, A. (1981). Extraocular muscle forces in normal human subjects. *Investigative Ophthalmology and Visual Science, 20,* 652–664.

Eshbach, O. W. & Souders, M. (1975). *Handbook of engineering fundamentals* (3rd edn). New York: Wiley.

Fuchs, A. F. & Luschei, E. S. (1970). Firing patterns of abducens neurons of alert monkeys in relationship to horizontal eye movement. *Journal of Neurophysiology, 33,* 382–392.

Fuchs, A. F., Kaneko, C. R. S. & Scudder, C. A. (1985). Brain stem control of saccadic eye movements. *Annual Review of Neuroscience, 8,* 307–337.

Goldstein, H. P. (1983). The neural encoding of saccades in the rhesus monkey. Ph.D. thesis, Johns Hopkins University, Baltimore, Md.

Goldstein, H. P. & Robinson, D. A. (1986). Hysteresis and slow drift in abducens unit activity. *Journal of Neurophysiology, 55,* 1044–1056.

Hepp, K. & Henn, V. (1985). Iso-frequency curves of oculomotor neurons in the rhesus monkey. *Vision Research, 25,* 493–499.

Judge, S. J., Richmond, B. J. & Chu, F. C. (1980). Implantation of magnetic search coils for measurement of eye position: An improved method. *Vision Research, 20,* 535–538.

Keller, E. L. (1980). Oculomotor specificity within subdivisions of the brain stem reticular formation. In Hobson, J. A. & Brazier, M. A. B. (Eds), *The reticular formation revisited* (pp. 227–240). New York: Raven Press.

Lehman, S. L. & Stark, L. (1983). Multipulse controller signals. III. Dynamic overshoot. *Biological Cybernetics, 48,* 9–10.

Miller, J. M. (1989). Functional anatomy of normal human rectus muscles. *Vision Research, 29,* 223–240.

Miller, J. M. & Robins, D. (1987). Extraocular muscle sideslip and orbital geometry in monkeys. *Vision Research, 27,* 381–392.

Miller, J. M. & Robinson, D. A. (1984). A model of the mechanics of binocular alignment. *Computers and Biomedical Research, 17,* 436–470.

Miller, J. M., Demer, J. L. & Rosenbaum, A. L. (1990). Two mechanisms of up-shoots and down-shoots in Duane's syndrome revealed by a new magnetic resonance imaging (MRI) technique. In Campos, E. C. (Ed.), *Strabismus and ocular motility disorders* (pp. 229–234). London: Macmillan.

Nichols, M. F. & Hahn, A. W. (1987). Electrical insulation of implantable devices by composite polymer coatings. *Biomedical Sciences Instrumentation, 23,* 57–62.

Pfann, K. D., Miller, J. M. & Keller, E. L. (1991). Muscle dynamics during monkey saccadic eye movements and simulated saccadic eye movements. *IEEE Engineering in Medicine and Biology Society.* In press

Robinson, D. A. (1963). A method of measuring eye movement using a scleral search coil in a magnetic field. *IEEE Transactions on Bio-Medical Electronics, 10,* 137–145.

Robinson, D. A. (1964). The mechanics of human saccadic eye movement. *Journal of Physiology, London, 174,* 245–264.

Robinson, D. A. (1975). A quantitative analysis of extraocular muscle cooperation and squint. *Investigative Ophthalmology and Visual Science, 14,* 801–825.

Robinson, D. A. (1981). Control of eye movements. In Brooks, V. B. (Ed.), *The nervous system, handbook of physiology* (Vol. II, Part 2, Chap. 28, pp. 1275–1320). Baltimore, Md: Williams & Wilkins.

Robinson, D. A., O'Meara, D. M., Scott, A. B. & Collins, C. C. (1969). Mechanical components of human eye movements. *Journal of Applied Physiology, 26,* 548–553.

Salmons, S. (1969). The 8th international conference on medical and biological engineering—meeting report. *Biomedical Engineering, 4,* 467–474.

Schmidt, E. M., McIntosh, J. S. & Bak, M. J. (1988). Long-term implants of Parylene-C coated microelectrodes. *Medical and Biological Engineering and Computing, 26,* 96–101.

Scott, A. B. (1992). Adaptation of eye muscles to eye position. In preparation.

Searl, S. S., Metz, H. S. & Lindahl, K. J. (1987). The uses of sodium hyaluronate as a biologic sleeve in strabismus surgery. *Annals of Ophthalmology, 19,* 259–262.

Sherrington, C. S. (1894). Experimental note on two movements of the eye. *Journal of Physiology, London, 17,* 27–29.

Sindermann, F., Geiselmann, B. & Fischler, M. (1978). Single motor unit activity in extraocular muscles in man during fixation and saccades. *Electroencephalography and Clinical Neurophysiology, 45,* 64–73.

Tabary, J. C., Tabary, C., Tardieu, C., Tardieu, G. & Goldspink, G. (1972). Physiological and structural changes in the cat's soleus muscle due to immobilization at different lengths by plaster casts. *Journal of Physiology, 224,* 231–244.

Van Gisbergen, J. A. M., Robinson, D. A. and Gielen, S. (1981). A quantitative analysis of generation of saccadic eye movements by burst neurons. *Journal of Neurophysiology, 45,* 417–442.

Walmsley, B., Hodgson, J. A. & Burke, R. E. (1978). Forces produced by medial gastrocnemius and soleus muscles during locomotion in freely moving cats. *Journal of Neurophysiology, 41,* 1203–1216.

Weber, R. B. & Daroff, R. B. (1972). Corrective movements following refixation saccades: Type and control system analysis. *Vision Research, 12,* 467–475.

Williams, P. E. & Goldspink, G. (1973). The effect of immobilization on the longitudinal growth of striated muscle fibres. *Journal of Anatomy, 116,* 45–55.

Williams, P. E. & Goldspink, G. (1978). Changes in sarcomere length and physiological properties in immobilized muscle. *Journal of Anatomy, 127,* 459–468.

Acknowledgements—The authors are grateful for valuable discussions with Jim Maxwell of University of Rochester, John Porter of University of Kentucky Medical Center, Alan B. Scott and Dave Sparks of University of Pennsylvania. The manuscript had the benefit of aggressive reviews by Jay Edelman, Herschel Goldstein of Wills Eye Hospital, Steve Heinen and Ed Keller. Kerstin D. Pfann assisted with data analysis. Rich Miller programmed the experimental protocols, Al Alden designed and constructed the electronics, and Jim Brodale did the artwork. Bruce K. Smith wrote the experimental control software system. X-ray equipment and expertise was provided by Kirk L. Moon and Rich Rogers of the Radiology Department of California Pacific Medical Center. This study was supported by Grant EY06973 to J. M. Miller from the National Eye Institute, National Institute of Health, Bethesda, Maryland, by Core Facilities Grant EY06883, and by the Smith-Kettlewell Eye Research Institute.